



Adaptive histogram equalization with visual perception consistency

Qi Yuan, Shengkui Dai*

Xiamen Key Laboratory of Mobile Multimedia Communication, School of Information Science and Engineering, Huaqiao University, Xiamen 361000, China



ARTICLE INFO

Keywords:

Adaptive histogram equalization
Visual perception consistency
Objective optimal model
Gray resolution

ABSTRACT

Histogram equalization (HE) is a well-established method for image contrast enhancement due to its simplicity and effectiveness. However, it suffers from three main shortcomings, i.e., over-enhancement, under-enhancement and mean shift. To address these issues, this paper proposes a systematic scheme, that is, adaptive histogram equalization with visual perception consistency (AHEVPC). Firstly, a novel histogram correction model is designed to get the optimal controlling parameters, which specifically address the aforementioned issues of HE. Besides, considering the subjective perception of the initial output of the model, two strategies are proposed to make the enhanced image more natural and comfortable. Finally, histogram equalization is applied to the modified histogram. Extensive experimental results demonstrate that the proposed scheme is reasonable and effective, and outperforms several state-of-the-art methods in terms of subjective and objective metrics.

1. Introduction

Image enhancement significantly enhances the visual perception of digital images. In recent years, with the increasing demand for higher image resolution and the expectation to process a broader range of scenes, the efficiency and adaptability of image enhancement techniques face more substantial challenges [1,2,3]. Histogram, as a representation of image statistics, is not restricted by image resolution and different scenes. Consequently, traditional histogram equalization (HE) can quickly achieve image enhancement across diverse scenes. Its basic idea is to stretch the histogram nonlinearly through the cumulative distribution function (CDF) of the image, so that the resultant histogram tends to be uniformly distributed. However, uneven stretching of this method can lead to inadequate image enhancement, such as over-enhancement and under-enhancement. Moreover, it alters the average brightness of the image, which is detrimental when processing continuous images [4,5].

To address the shortcomings of traditional HE, many improved methods have been proposed, which can be categorized into two main directions: contrast enhancement and brightness control. Contrast enhancement strategies, such as histogram clamping [6], histogram weighting [7] and adaptive correction [8], have been used to solve the problems of over-enhancement and under-enhancement. Brightness control methods, including double histogram equalization and multi-histogram equalization [11,12,19], aim to address the problem of mean shift. However, neither approach can simultaneously resolve all the drawbacks of HE. Furthermore, these HE-based methods fail to take human vision system (HVS) into consideration [13,14,15], resulting in a mismatch between

* Corresponding author.

E-mail address: d.s.k@hqu.edu.cn (S. Dai).

the objective effect of the enhanced image and the subjective visual perception.

In this work, we propose a systematic solution to overcome all the limitations of HE. Firstly, we establish a novel objective model to address the three shortcomings of HE. This model features a mechanism to regulate the brightness of the output image by adjusting the CDF value of the input image average point. Secondly, to consist the model output with human visual perception, we introduce further enhancements through two strategies: adaptive brightness control and visual restriction, aiming to make the enhanced image more natural and comfortable. This scheme offers a novel perspective for improving HE algorithms. Numerous experiments have demonstrated that the proposed method shows superior performance over other methods, both in subjective and objective evaluations. In summary, the key contributions of this paper are three-fold:

- (1) Theoretically, we propose a new idea to achieve adaptive brightness preservation by controlling the CDF value of the input image average point to approach the quantile of the target brightness.
- (2) Methodologically, we develop a histogram correction model to automatically determine three adjustment parameters for the three shortcomings of traditional HE.
- (3) In terms of effectiveness, our scheme integrates the characteristics of human vision to ensure the objective effect of the model output consistent with subjective human perception.

The remainder of this paper is organized as follows: Section 2 reviews related work. Section 3 describes the detailed procedures of our proposed scheme. Section 4 shows experimental results and quality evaluations. Section 5 concludes the paper.

2. Related work

The histogram is a graph with gray value and the number of pixels as the horizontal axis and the vertical axis, respectively. It is obtained by counting the number of pixels of each gray value present in the image. To represent the proportion of each gray level within the image, probability distribution histogram h is calculated by scaling down the vertical axis of the histogram in proportion to the total number of pixels. The probability distribution histogram is then multiplied by the gray value variation range, L , to satisfy the gamma correction curve. This adjustment ensures that both horizontal and vertical coordinates change within the range $[0, L]$. The expression is as follows:

$$hist = h \times L \quad (1)$$

where $hist$ represents the mean normalized histogram. The mean value of the pixel count in the updated histogram is also scaled to 1 by a factor of L , which facilitates a precise definition of the pixel numbers. The gray levels with $hist$ less than 1 are referred to as small data. The cumulative distribution function (CDF) is obtained by integrating h , which is employed as a conversion function to equalize the histogram and make the histogram evenly distributed. However, histogram equalization (HE) suffers three main shortcomings, i.e., over-enhancement, under-enhancement and mean shift. Addressing these limitations has been a hot research topic [16,17,18], with major improvement efforts concentrated on contrast enhancement and brightness control.

Contrast enhancement methods have been developed to address the shortcomings of over-enhancement and under-enhancement [29,31]. Among these, quadrants dynamic histogram equalization (QDHE) [27] and exposure-based sub-image histogram equalization (ESIHE) [28] were introduced to control the rate of contrast enhancement. These methods segment the histogram based on the mean brightness and exposure threshold, respectively. While ESIHE lacks sufficient enhancement for local details, it is easier to implement compared to QDHE. Furthermore, Hajinorozi et al. proposed an image enhancement method called weighted histogram equalization (WHE) [30], which adjusts the histogram before equalization by applying a weight to each gray level. This approach effectively reduces the stretch degree of the histogram and the merging of gray levels, but the fixed parameters limit its adaptability to different images. Therefore, to adaptively determine parameters for global adjustment, Rahman et al. proposed adaptive gamma correction (AGC) [32], which dynamically adjusts its parameters based on the specific information of each image. This method significantly enhances the luminance of dimmed images but fails to achieve enough overall contrast. In [33], a ramp distribution-based slant thresholding (RDST) method is proposed, which utilizes the ramp distribution function to modify the global ascending. RDST aims to prevent the unnatural appearance associated with excessive enhancement, but its effectiveness is highly dependent on the adaptive threshold.

Brightness control methods have been specifically designed to address the shortcoming of mean shift. Kim firstly proposed brightness preserving bi-histogram equalization (BBHE) [9], which divides the histogram into two sub-histograms based on the mean brightness of the input image prior to equalization. Subsequently, Wang et al. developed a similar method called dualistic sub-image histogram equalization (DSIHE) [10], using the median value as a segmentation criterion instead of mean brightness. However, both methods exhibit limitations in their ability of brightness preservation. Recursively separated and weighted histogram equalization (RSWHE) [20] introduces histogram weighting module and applies a normalized power law function for sub-histogram modification, thereby enhancing brightness preservation. However, the increased computational complexity presents a significant drawback. In recent years, studies on brightness preservation are still emerging [21,22,23]. In 2019, Park et al. introduced a sensitivity model-based sigmoid function (SMBSF) [24] to maintain the mean brightness of the input image, where the optimal parameter was determined by the golden section search algorithm [25]. In 2020, Singh et al. proposed a method using an optimal gamma and logarithmic approach (BPLGA) [26], in which gamma and logarithmic transformations are adopted to adjust the input histogram before its segmentation.

In addition to the previous discussed methods, alternative approaches [34,35] have been developed to enhance histogram

equalization, such as the contrast enhancement using combined 1-D and 2-D histogram-based techniques (COTH) [36]. This technique utilizes the statistical information captured by 2-D histogram to refine image details while preserving the shape of the 1-D histogram. Furthermore, a contextual and variational contrast enhancement (CVC) method has been introduced [37], which enhances the local details by amplifying the gray level differences between adjacent pixels. Compared to methods relying solely on 1-D histograms, the application of 2-D histograms offers a significant reduction in visual distortion of the output image, but it increases the computational complexity. At present, the high-resolution image and video produced by electronic equipment has placed more stringent demands on the performance capabilities of image processing techniques. Consequently, deep learning-based methods [38,39,40], especially those involving deep neural networks (DNN), have increasingly been employed.

3. Proposed systematic scheme

Firstly, the core principle of the proposed scheme is to ensure that the mean of the output image is close to the set target value by controlling the CDF value of the input image average point. Specifically, the scheme comprises three integral components. The first part, termed the CDF-based model, aims to overcome the three shortcomings inherent in histogram equalization. It has three adjustment steps to modify the histogram under the basic rule. Subsequently, the second component is designed to further adjust the histogram in order to make the output image match the subjective perception of HVS. The last component equalizes the adjusted histogram to get the final enhanced image. The process is shown in Fig. 1.

3.1. Histogram correction with CDF-based model

3.1.1. Initial adjustment based on the traversal

To address the shortcomings of HE related to both contrast and brightness concurrently, an adjustment coefficient, with brightness serving as the constraint condition for gamma correction, must be carefully selected. The constraint on brightness is achieved by controlling the mean of the output image. This is accomplished by multiplying the CDF value of the input image average point I_m by the dynamic range L of the gray level, thereby mapping the mean of the input image to that of the output image. As a result, the mean of the output image can be controlled by the CDF value of I_m .

Herein, the histogram is segmented at the mean value of the input image (I_m) into two components: the left and right sub-histograms. The sum of the pixels in the left sub-histogram is denoted as N_l , and N_t represents the sum of the pixels in the entire histogram. These values are used to calculate the CDF value of I_m . The adjustment coefficient γ is selected based on the traversal, with the traversal range from 0 to 1. The objective function is designed as follows:

$$\Delta = \underset{\gamma}{\operatorname{argmin}} \{ |CDF(I_m) - \lambda|, \quad \gamma \in [0, 1] \} \quad (2)$$

$$s.t. \quad CDF(I_m) = \frac{N_l}{N_t}, \lambda = \frac{I_t}{255} \quad (3)$$

where I_t is the set target mean of the output image depending on the brightness requirements. Here I_t is 127. λ is the quantile of I_t in the dynamic range L . The CDF value of I_m and λ are in the range of [0, 1]. The objective function is to minimize the difference (Δ) between the CDF value of I_m and λ by traversing different gamma values from 0 to 1, in which case the corresponding gamma value is the sought adjustment coefficient (γ_1). The adjusted function is formulated as:

$$hist_1(k) = hist(k)^{\gamma_1} \quad (4)$$

where γ_1 is used as global correction parameter for the mean normalized histogram (hist). Adjusted histogram ($hist_1$) makes the equation true, that is, $CDF(hist_1, I_m) = \lambda$.

Fig. 2 illustrates the traversal optimization process. Fig. 2(a) and (b) shows the statistics and difference of the CDF value of I_m and λ , respectively. It is evident that the optimal gamma value, which minimizes the difference, is approximately 0.55. To provide a benchmark, the histograms of the original image with and without initial adjustment are depicted in Fig. 2(c). It is clearly observable that the gray levels with $hist > 1$ are significantly weakened, while the small data, the gray levels with $hist < 1$, is slightly improved. As demonstrated in Fig. 3(c), the contrast in the underexposed regions in Fig. 3(a) is effectively enhanced, and the

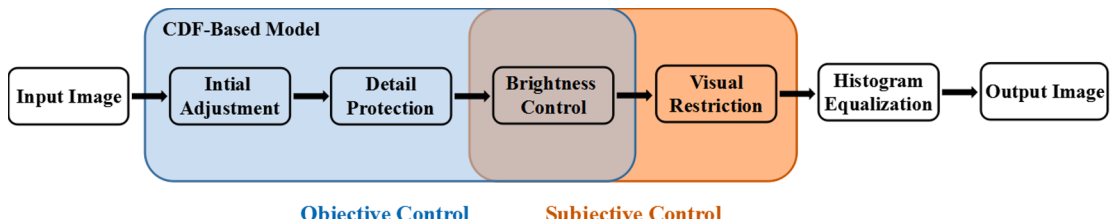


Fig. 1. Framework of the proposed scheme.

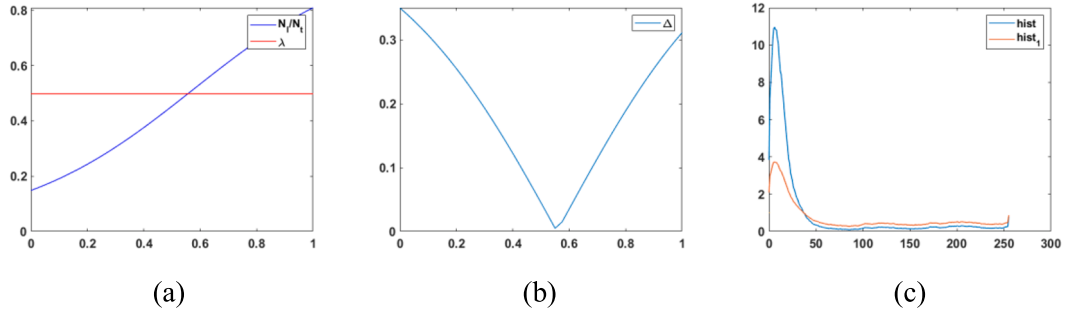


Fig. 2. The process of traversal optimization to get γ_1 .

intensity saturation effect depicted in Fig. 3(b) is fully alleviated. This comparison underlines the efficiency of the proposed initial adjustment in enhancing image contrast, particularly in areas of low exposure, while concurrently alleviating issues of intensity saturation, thereby achieving a more balanced and visually pleasing image output.

To demonstrate the effectiveness of the initial adjustment in controlling the brightness, two sets of images including the input images and the processed images with varying target average values, are presented in Fig. 4. As presented in Fig. 4(a), the input image is an extremely dark image. When target mean value I_t is set at 77 or 127, the mean value of the image is adjusted to 73.4 or 114.4, respectively. The corresponding relative errors for these adjustments are 0.047 and 0.099. For the bright image shown in Fig. 4(d), when I_t is set at 177 or 127, the mean value of the image is adjusted to 176.5 or 139.0, respectively, with corresponding relative errors of 0.003 and 0.094. The results indicate that the initial adjustment can effectively control the brightness of the processed image to reach the target brightness.

3.1.2. Detail protection

Due to the discreteness of gray levels in digital images, the gray levels of the original image with low probabilities are easier to be lost after the initial adjustment. Therefore, a secondary gamma correction is only applied to the small data. The processing function is defined as:

$$hist_2 = \begin{cases} hist_1, & hist_1 \geq 1 \\ hist_1^{\gamma_2}, & hist_1 < 1 \end{cases} \quad (5)$$

where $hist_1 = 1$ (the mean value of the pixel count) is used to distinguish between large and small data. γ_2 is the coefficient of secondary gamma correction for the small data. To make both γ_1 and γ_2 vary from 0 to 1, γ_2 is calculated as:

$$\gamma_2 = \alpha \times (1 - \gamma_1) \quad (6)$$

where $\hat{I} \pm$ is the weight coefficient and the default value is 1. γ_2 is inversely proportional to γ_1 . A larger γ_1 signifies minimal improvement of the initial adjustment on the small data, hence a smaller γ_2 is employed to augment these data significantly, thereby better preserving detailed features.

Fig. 5 compares the image process outcomes with and without the implementation of detail protection. The obvious area is marked with a red box. Although the initial adjustment effectively enhances the overall brightness and contrast of the original image, the texture details on the door handle are not well maintained. In sharp contrast, as shown in Fig. 5(c), the detail protection mechanism

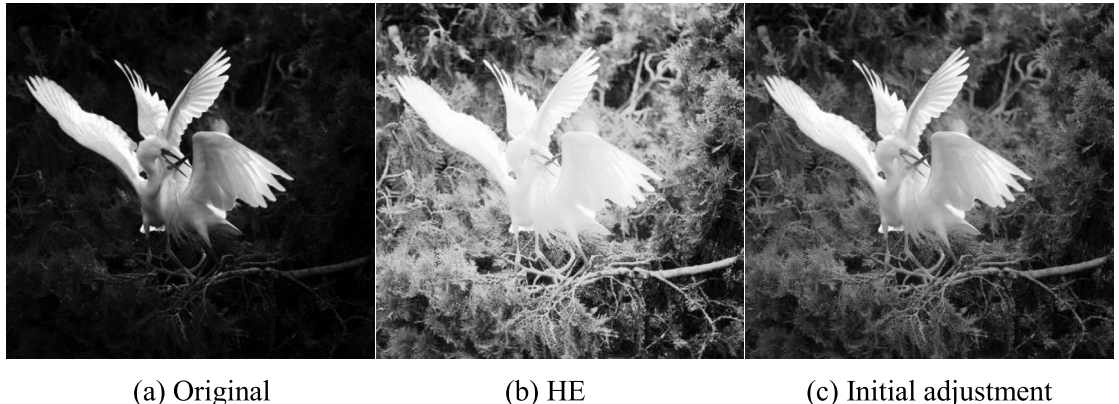


Fig. 3. Comparison of three images. (a) The original image. (b) The enhanced images using HE and (c) initial adjustment.

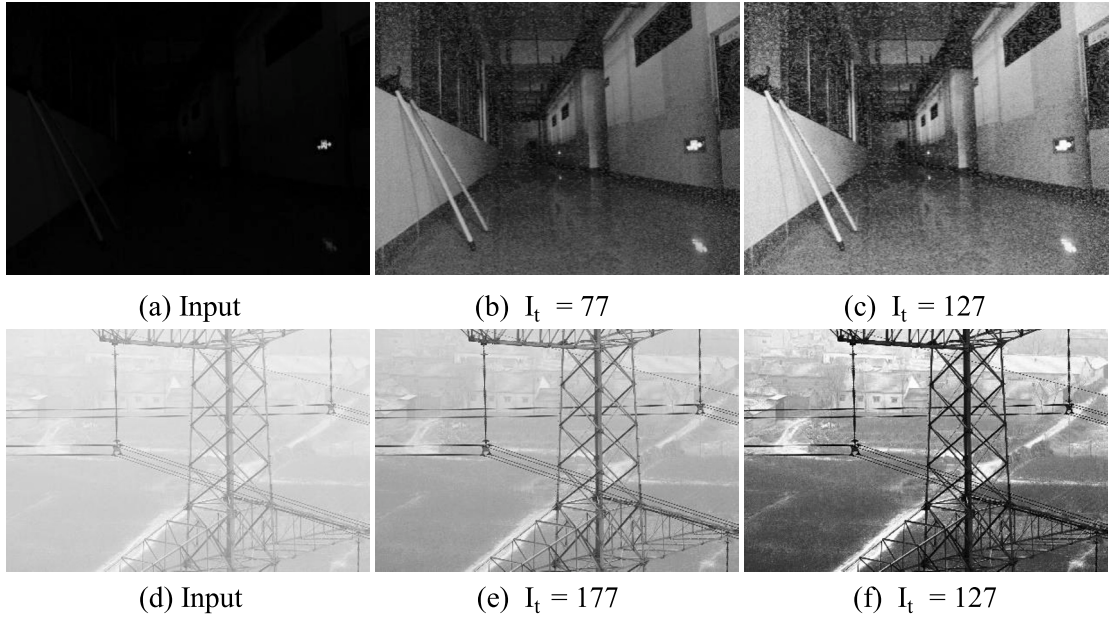


Fig. 4. Processed images corresponding to different target average values.

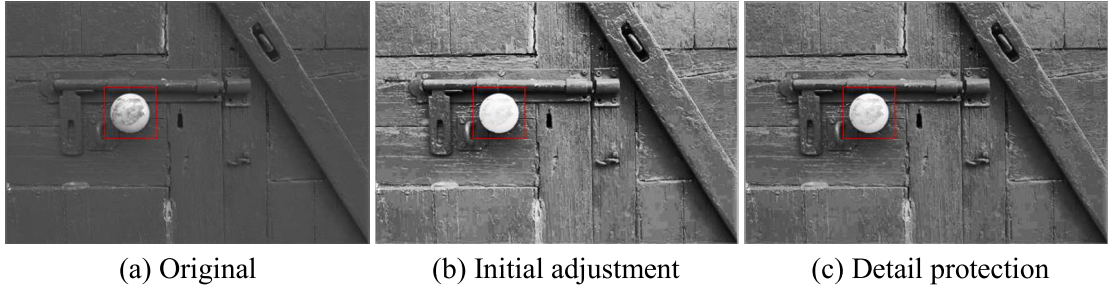


Fig. 5. Comparison of three images. (a) The original image. (b) The enhanced images with and (c) without detail protection.

results in clearer and more pronounced texture details within the marked area compared to that in Fig. 5(b).

3.1.3. Brightness control

The second adjustment for the histogram is crucial for protecting the details from under enhancement, but its side effect is a violation of the basic rule. The initial equation, $CDF(hist_2, I_m) = \hat{I}$, is no longer valid. Therefore, a luminance adjustment factor is introduced to correct $hist_2$. This factor is strategically applied based on the relationship between the CDF value of I_m and \hat{I} . Specifically, when the CDF value of I_m is less than \hat{I} , indicating that the mean brightness of the original image would be mapped to a darker range, a corrective bias is added to the left non-zero portion of the histogram. The adjusted histogram ($hist_3$) satisfies that $CDF(hist_3, I_m) = \hat{I}$ and vice versa, that is:

$$hist_3(k_l) = hist_2(k_l) + \delta_1, \text{ when } CDF(I_m) \leq \lambda \quad (7)$$

$$hist_3(k_r) = hist_2(k_r) + \delta_2, \text{ when } CDF(I_m) > \lambda \quad (8)$$

where k_l and k_r are the index values of the left non-zero histogram and right non-zero histogram, respectively. δ_1 and δ_2 are added biases for brightness control compensation, which can be derived from formula (3), (7), (8) and equation $CDF(hist_3, I_m) = \hat{I}$ as follows:

$$\delta_1 = \frac{I_l \times hist_l - 255hist_l}{k_l \times (255 - I_l)} \quad (9)$$

$$\delta_2 = \frac{255hist_l - I_l \times hist_l}{k_r \times I_l} \quad (10)$$

where hist_l and hist_t represent the left sub-histogram and the total histogram, respectively. I_t is the target average value 127.

Fig. 6 illustrates the processing effect at each stage within the entire CDF-based model, with corresponding mean values of 118.6, 101.6 and 119.4. It is observable that the image becomes darker after detail protection, thus increasing the deviation from the target average value of 127. As shown in **Fig. 6(c)**, the implementation of the brightness control compensation term brings the image's mean value close to the target mean once again, while also yielding a slight improvement in the image's contrast.

3.2. Subjective control

Model-based enhancement effectively addresses the three principal shortcomings of HE and achieves controllable target brightness. However, the actual effect of the model occasionally diverges from the subjective perception of the HVS. Consequently, we propose further refinements from two distinct perspectives to align the enhanced images more closely with human visual perception.

3.2.1. Adaptive brightness control

For low exposure and high brightness images, when the target brightness is set unreasonably, the processed image effect is inconsistent with the human visual perception. To address this discrepancy and enhance consistency with human visual perception, we propose the introduction of a weighting factor to adaptively adjust the bias. The empirical formula is given by:

$$\omega = \exp \frac{-(I_m - I_t)^2}{2\sigma^2} \quad (11)$$

where σ defaults to 30, ω is used as the weight of the above δ_1 and δ_2 . The processing effects are shown in **Fig. 7**. The mean value of the original image is 4.3, which are adjusted to 107.1 and 79.0 without and with weighting, respectively. Compared with **Fig. 7(b)**, the overall brightness in **Fig. 7(c)** is more natural.

3.2.2. Visual restriction based on the visual perception curve

For some extremely dark or extremely bright images, the objective model cannot well suppress histogram spikes, leading to poor image effects. To mitigate this issue, the introduction of a visual perception curve is proposed to effectively truncate the histogram. The just noticeable difference (JND) curve [41] is a common visual curve that reflects the minimum brightness deviation detectable by the human eye against a specific background. Besides, subsequent experiments and tests [42] have demonstrated that the gray resolution of the human eye, Rg , and the gray level, g , can be approximately expressed by piecewise function as:

$$Rg = \begin{cases} -g/8 + 6, & 0 \leq g < 32 \\ -g/32 + 3, & 32 \leq g < 64 \\ g/128 + 0.5, & 64 \leq g < 192 \\ g/64 - 1, & 192 \leq g < 256 \end{cases} \quad (12)$$

As shown in **Fig. 8**, both curves indicate that the gray resolution of human eye diminishes at both high and low gray levels. However, the Rg curve provides a more accurate division of the histogram into four distinct segments compared to the JND curve. Therefore, the histogram of the CDF-based model output (hist_3) is restricted based on the Rg curve to suppress histogram spikes. To achieve a better restriction effect, the truncation threshold and the corresponding operation are as follows:

$$Th = aRg + b \quad (13)$$

$$\text{hist}_4 = \min(\text{hist}_3, Th) \quad (14)$$

where a and b are used to control the slope and height of the Rg curve, respectively. The default experience values are 2 and 5. The final histogram hist_4 takes the minimum values of hist_3 and Th .

Fig. 9 showcases the comparative processing effects with and without the implementation of visual restrictions. As demonstrated in

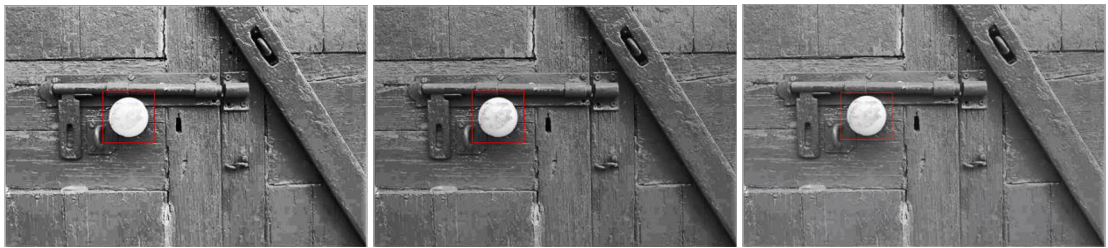


Fig. 6. The processing effect of each step of the proposed model.

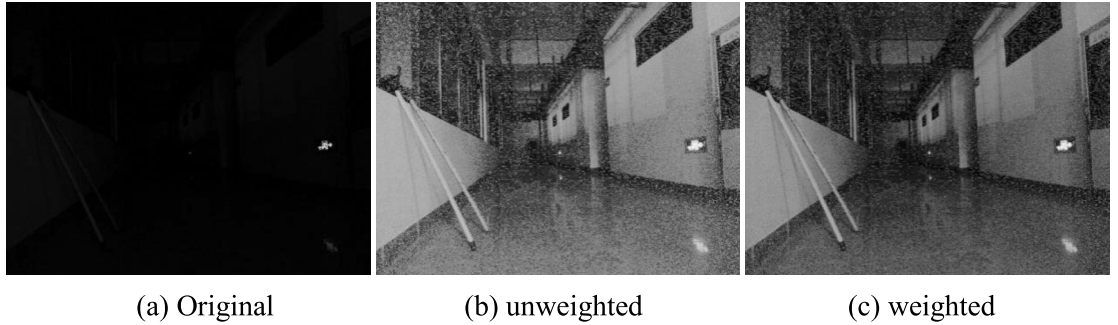


Fig. 7. Comparison of three images. (a) The original image. (b) The enhanced images without and (c) with weighting.

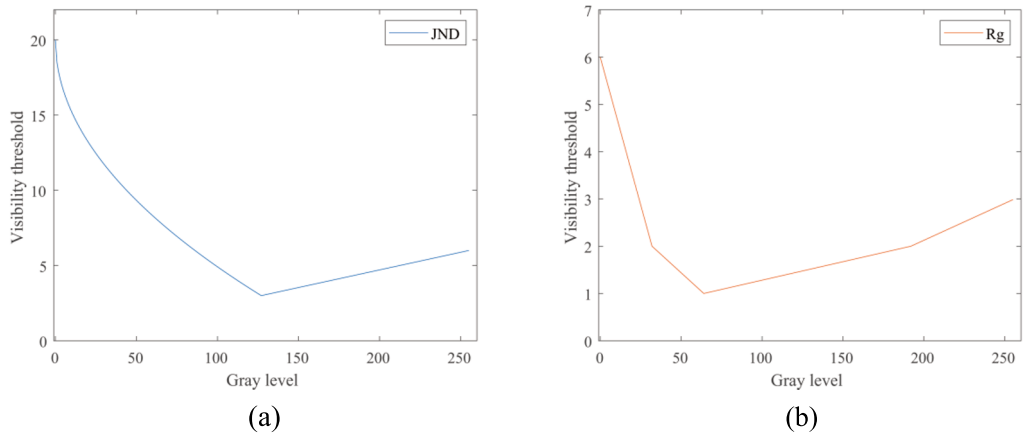


Fig. 8. The relationship between the visibility threshold and the gray level reflected by (a) the JND curve and (b) the Rg curve.

Fig. 9(b), while the brightness and contrast of the original image are significantly enhanced through our objective model, the excessive brightness of the background detracts from the prominence of the target. Conversely, in **Fig. 9(c)**, the application of visual restrictions effectively moderates the background brightness, resulting in an outcome that more closely aligns with human visual perception. This adjustment ensures that the target within the image is adequately highlighted, enhancing the overall visual appeal and interpretability of the image in accordance with the nuances of human vision.

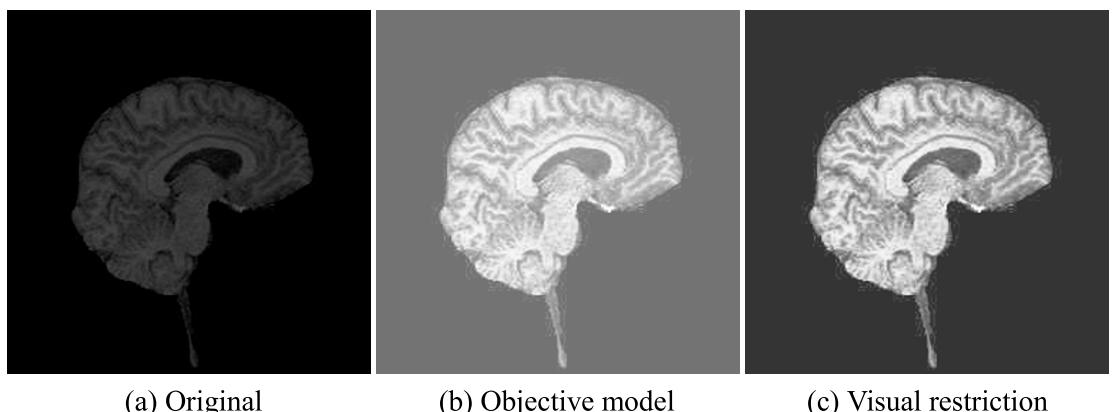


Fig. 9. Comparison of three images. (a) The original image. (b) The enhanced images with and (c) without visual restriction.

4. Experimental results and analyses

In this section, we conduct a subjective and objective comparison of the proposed AHEVPC against several leading-edge methods, including ESIHE [28], WHE [30], AGC [32], RDST [33], SMBSF [24], and BPGLA [26]. All experiments are performed using MATLAB 2016 on a computer running Windows 7, equipped with 12 GB of RAM and a 3.4 GHz CPU. A variety of typical images and several image databases are utilized for evaluation, encompassing scenarios such as low-light images, non-uniform illumination images, and indoor images, all assessed within the HSV color space. This comprehensive approach ensures a robust comparison across a broad spectrum of visual conditions, highlighting the efficacy of the AHEVPC method in enhancing image quality in alignment with human visual perception.

The proposed AHEVPC algorithm is implemented as follows:

Algorithm

-
- Step 1: Input an image and get its mean normalized histogram hist using Formula (1).
 - Step 2: Find the best global correction parameter γ_1 for hist using Formula (2) and (3), thereby obtaining the adjusted histogram hist₁ by Formula (4).
 - Step 3: Calculate the coefficient of secondary gamma correction γ_2 using Formula (6).
 - Step 4: Adjust small data in hist₁ to obtain hist₂ using Formula (5).
 - Step 5: Calculate brightness bias δ_1, δ_2 and weighting factor ω using Formula (9), (10) and (11).
 - Step 6: Obtain the histogram of the CDF-based model output hist₃ using Formula (7) and (8).
 - Step 7: Calculate truncation threshold Th using Formula (13) and obtain truncated histogram hist₄ by Formula (14).
 - Step 8: Equalize hist₄ to obtain enhanced image.

4.1. Subjective visual evaluation

The visual comparison across seven enhancement methods is illustrated through four sets of images, with particular focus on zoomed-in sections to critically assess their subjective quality. In Fig. 10(a), depicting a low-light image of a swan, the essence of enhancement lies in preserving the original details. The zoomed-in areas reveal that the details on the swan become blurred in Fig. 10 (c) and (d), with WHE causing an undue increase in brightness. Conversely, ESIHE, SMBSF, and BPGLA inadequately enhance brightness, rendering the water waves indistinct. RDST outperforms the aforementioned methods. However, its visual effect is still not as satisfactory as AHEVPC, primarily due to over-enhancement. Fig. 11 presents the “Marsh” image, which originally suffers from low contrast, alongside the enhancements rendered by different methodologies. The enlarged views demonstrate that ESIHE and SMBSF fall short in augmenting brightness. AGC and BPGLA exhibit comparable performances, yet neither sufficiently boosts the overall contrast, leading to obscured details. RDST and WHE, while striving for enhancement, inadvertently obscure details through over-enhancement. AHEVPC, in contrast, achieves an optimal balance between brightness and contrast, closely aligning with human visual perception and outshining its counterparts in rendering a balanced and visually appealing image.

Fig. 12 demonstrates the enhanced results of the image “House”, which is a backlit image where the sky in the distance is normal

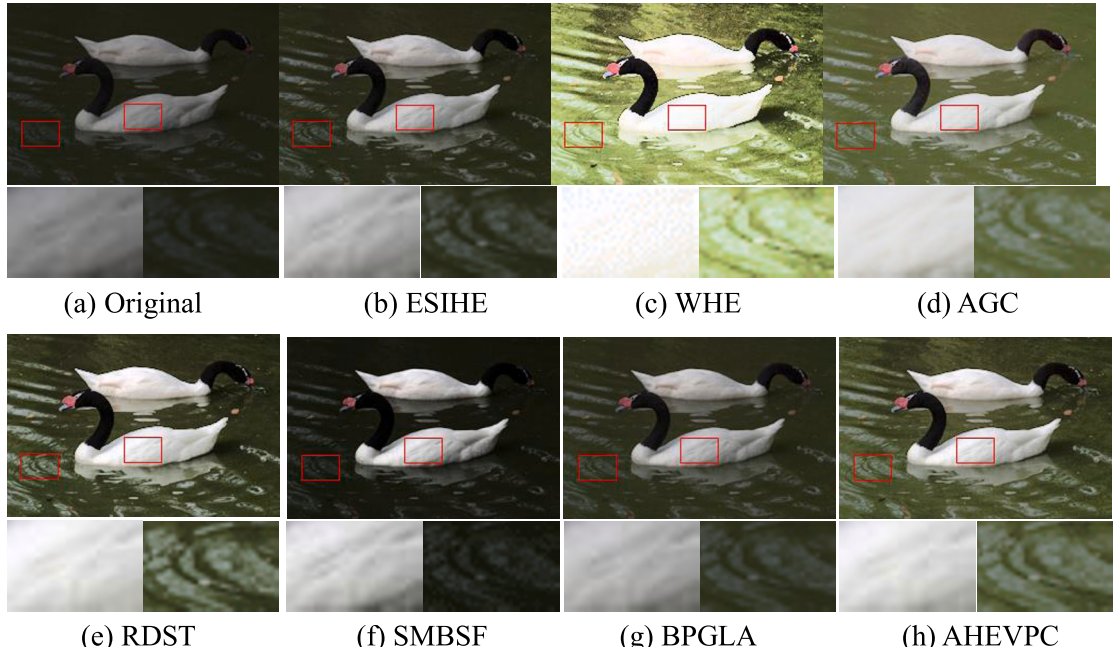


Fig. 10. Enhanced results of the image Swan.

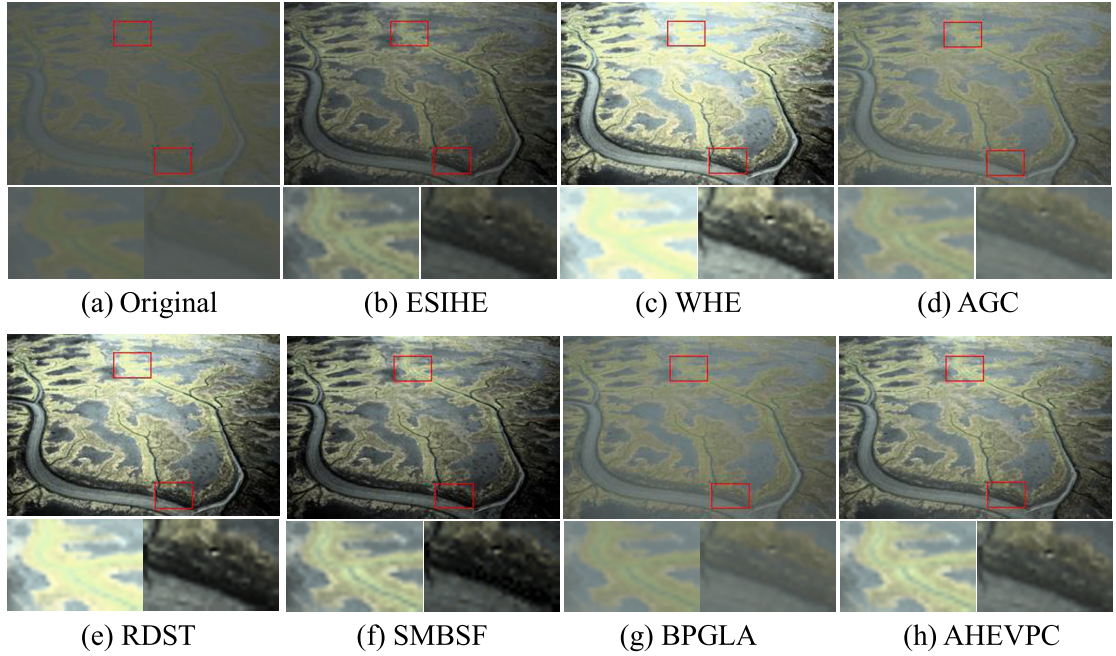


Fig. 11. Enhanced results of the image Marsh.

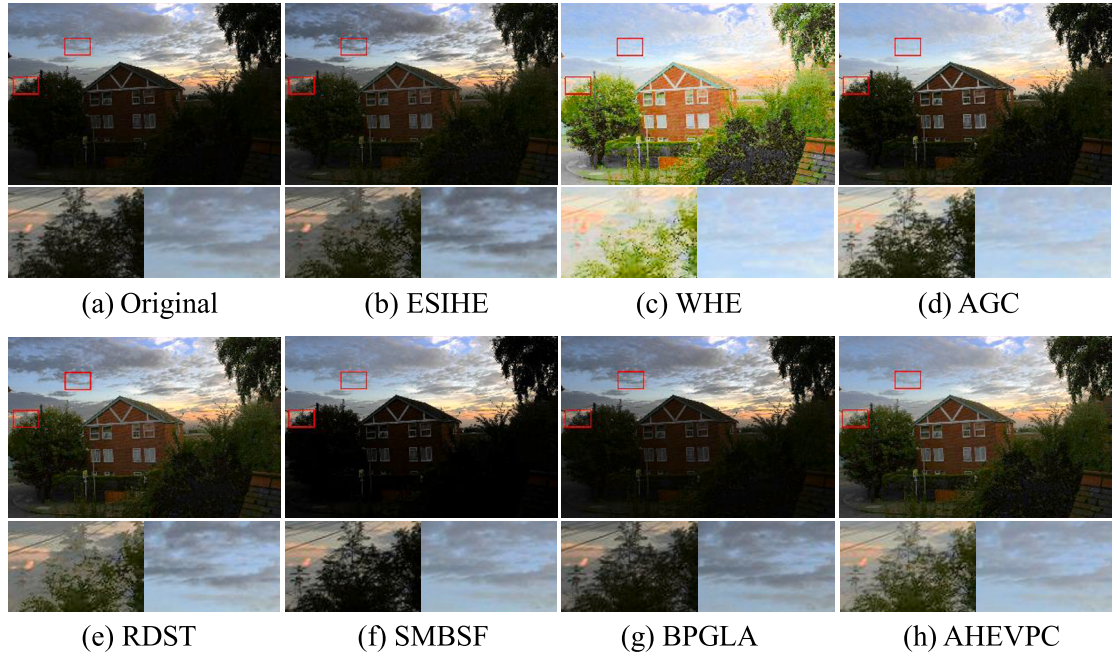


Fig. 12. Enhanced results of the image House.

but the close details are masked. ESIHE, SMBSF, and BPGLA demonstrate limited efficiency in enhancing the details of nearby houses and trees. WHE significantly increases the brightness but inevitably produces an unnatural appearance. The zoomed-in sections reveal that AGC does not adequately preserve the cloud textures, and there is a need for further enhancement of the foreground brightness. RDST results in contour artifacts, while AHEVPC effectively improves the brightness with distinct edges. Fig. 13 presents a visual comparison of the seven methods applied to the image "Woman." The foreground of the original image is so brightly illuminated that it results in a visual dilution effect, which AGC fails to adequately address. In the enhancements rendered by WHE, RDST, and SMBSF, the scarf's fringe details remain indistinct. Moreover, RDST causes the woman's hair to appear unnaturally black due to excessive contrast

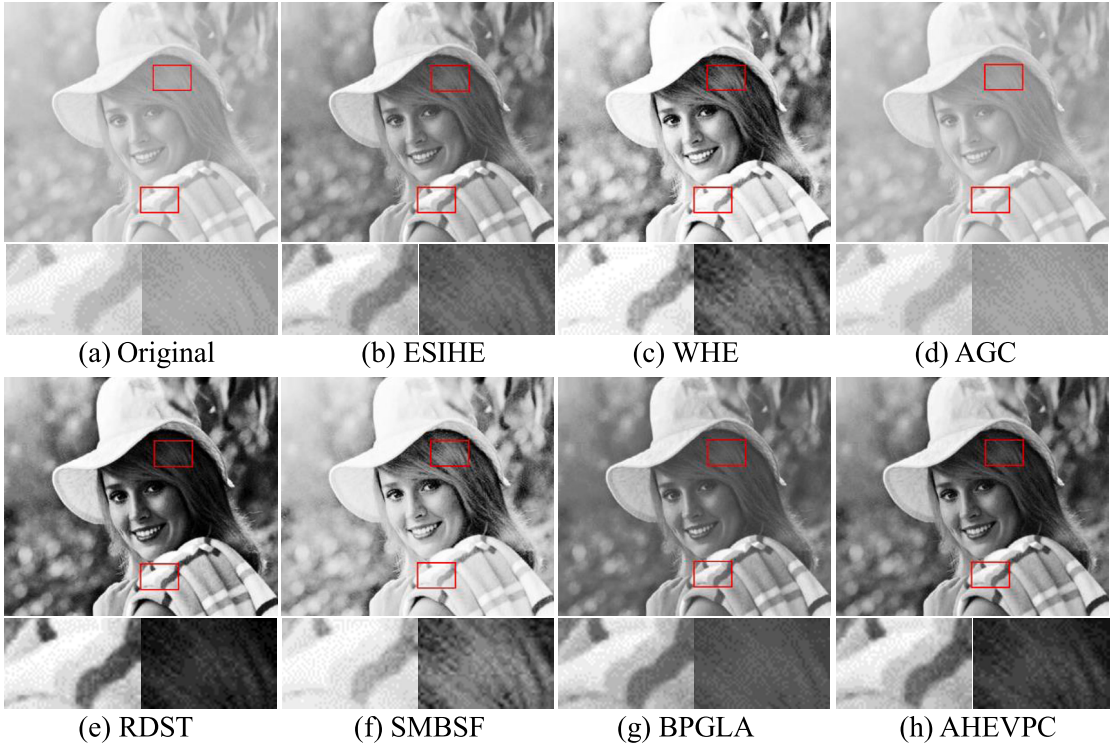


Fig. 13. Enhanced results of the image Woman.

enhancement. In comparison, AHEVPC not only provides superior brightness enhancement but also meticulously preserves the scarf's details, showcasing its effectiveness over BPGLA in achieving a balanced and detail-preserving enhancement that aligns more closely with human visual perception.

Moreover, Fig. 14 facilitates a comparison between the proposed method and Deep Neural Network (DNN)-based methods, specifically the Deep Photo Enhancer (DPE) [40] and Deep Local Parametric Filters (DeepLPF) [39]. The input images and their corresponding results are derived directly from the original publications. As evidenced in Fig. 14(c), the results produced by our traditional method are competitive, with the noticeable difference in color primarily attributed to the absence of color correction in our approach. Fig. 15 further showcases a broader array of experimental outcomes achieved by the proposed AHEVPC underscoring its versatility and effectiveness across various imaging scenarios. These results illustrate the capability of AHEVPC to deliver high-quality image enhancement.

4.2. Objective quality assessment

Only considering the visual quality of an image for evaluation is insufficient to conclusively determine whether its quality has been enhanced. Therefore, a mathematical evaluation is required to identify the enhancement of the image quality. Herein, we employ three quality metrics to evaluate our method: Naturalness Image Quality Evaluator (NIQE), Perception based Image Quality Evaluator (PIQE), and Maximize Contrast with Minimum Artefact (MCMA). Each of these metrics provides a unique perspective on image quality, as described below:

- (1) Naturalness Image Quality Evaluator (NIQE): This metric is based on natural image statistics and generalized Gaussian model. The distance between the parameters of the image feature model to be evaluated and the parameters of the pre-established model is used to evaluate the image quality. The calculation formula is as follows [43]

$$D\left(v_1, v_2, \sum_1, \sum_2\right) = \sqrt{\left(v_1 - v_2\right)^T \left(\frac{\sum_1 + \sum_2}{2}\right)^{-1} \left(v_1 - v_2\right)} \quad (15)$$

where v_1, v_2 and \sum_1, \sum_2 are the mean vectors and covariance matrices of MVG models of natural and distorted image, respectively. The smaller the NIQE value is, the better the image naturalness will be.

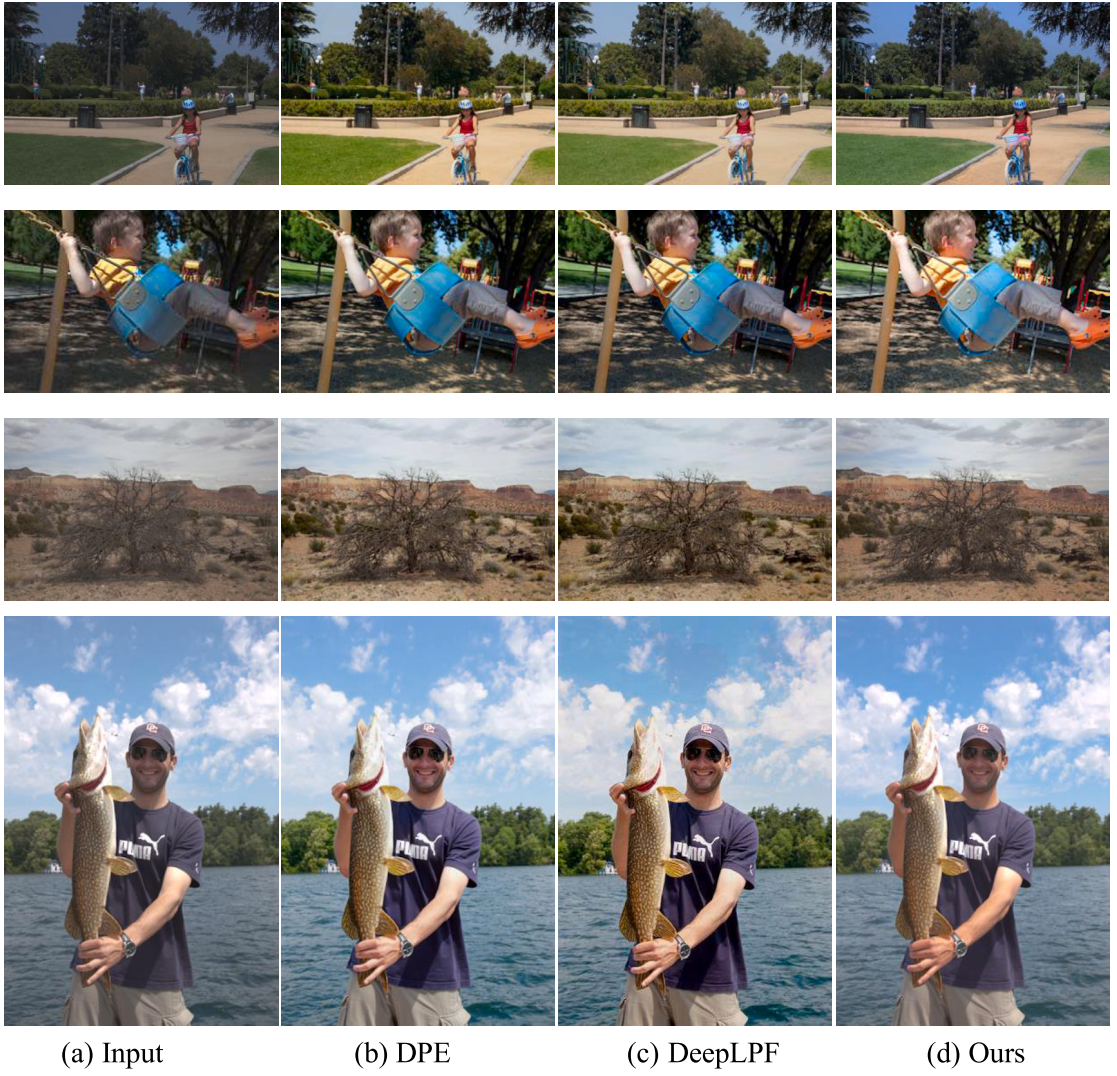


Fig. 14. Additional comparison between DNN-based methods and our method.

(2) Perception based Image Quality Evaluator (PIQE): This is a kind of no-reference image quality evaluation index, which combines the perception characteristics of human eyes. The algorithm evaluates the significant area of the image and gets the noise and blur degree of the image. The calculation formula is as follows [44]

$$PIQE = \left(\left(\sum_{k=1}^{N_{SA}} D_{sk} \right) + C_1 \right) / (N_{SA} + C_1) \quad (16)$$

where D_{sk} is the distortion degree of the local image, that is, the variance of MCSN. N_{SA} is the number of the effective local image blocks and C_1 is a constant. A lower PIQE value represents a higher image quality.

(3) Maximize Contrast with Minimum Artefact (MCMA): This metric is built upon three sub-measures including dynamic range occupation (DRO), histogram shape deformation (HSD) and pixel uniformity (PU). They have been proven to be loosely correlated to the perceived contrast-based quality, yet they do not individually cover all possibilities for contrast degradation. Therefore, efficiently combining these three sub-measures in such a way could quantify contrast quality more reliably. The calculation formula is as follows [45]

$$MCMA = 0.71 \times (0.4 \times P_{DRO} - 0.3 \times P_{HSD} - 0.7 \times P_{PU} + 1) \quad (17)$$

where P_{DRO} , P_{HSD} and P_{PU} are the dynamic range of the image, the similarity of the global histogram and the local pixel richness of the image, respectively. The larger the MCMA index is, the better image contrast quality will be.

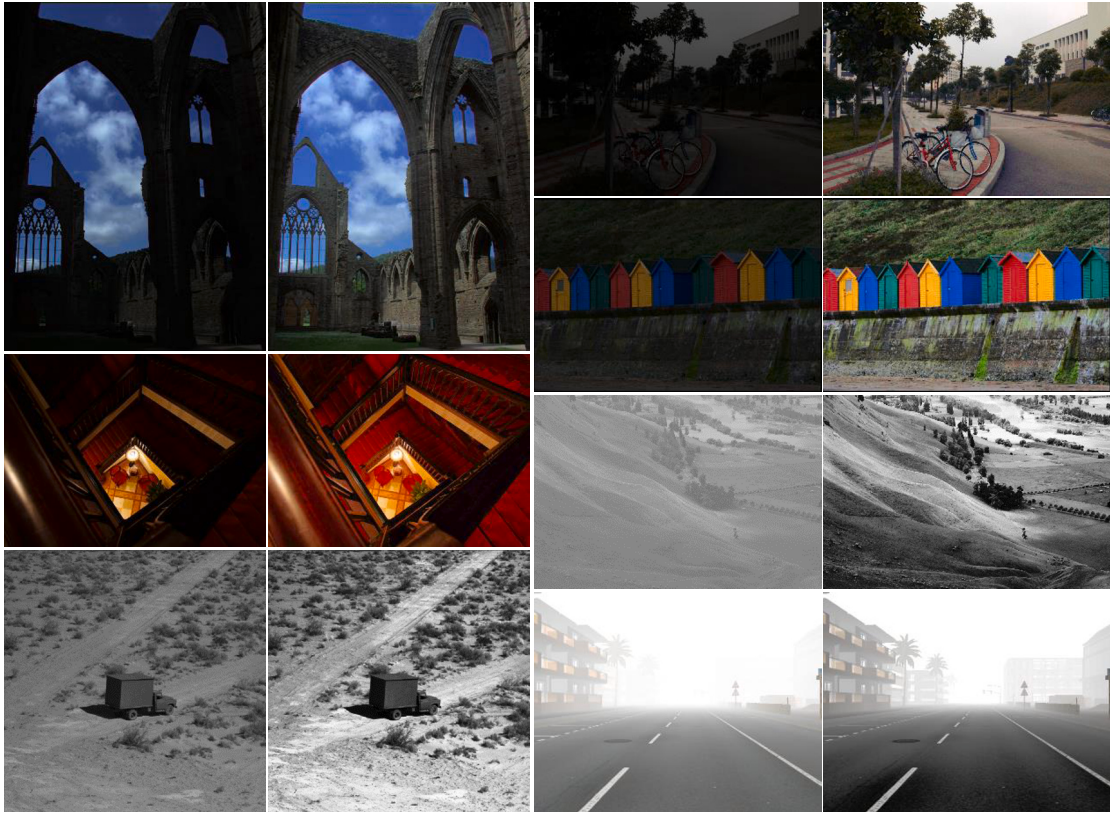


Fig. 15. More results by the proposed AHEVPC.

Three quality metrics of the images in Figs. 10–13 are shown in Table 1, where the bold numbers represent the optimal values of the evaluation algorithm and suboptimal values are underlined. In order to make our evaluation results more general, we randomly test 220 images from five public databases, which include USC-SIPI [46], LIME [47], BSR Berkeley [48], NPE [49], and FiveK [50]. Here, we introduce the box plots to illustrate the comparison results of different metrics in Fig. 16. As can be seen from the box plots, AHEVPC has the lowest average for NIQE and PIQE, which indicates that the enhanced images have the most natural appearance, minimum noise and distortion. Moreover, the performance of AHEVPC on MCMA is also the best. Therefore, our proposed AHEVPC can achieve more desirable visual quality than other methods.

To illustrate the computational complexity of the proposed algorithm, Table 2 and Table 3 present the processing time of the proposed algorithm and various algorithms in processing different images, respectively. The test images come from this paper, and the experimental results are averaged ten times. As shown in Table 2, the larger the image size, the longer the processing time, and it only takes 29 ms to process a 1556×1037 size image. Table 3 shows that the proposed algorithm exhibits low computational complexity for

Table 1

The assessment results for test images in Figs. 10–13 in terms of three quality metrics.

Image	Metric	Original	ESIHE	WHE	AGC	RDST	SMBSF	BPLGA	Proposed
Swan	NIQE↓	7.55	7.02	7.02	6.55	<u>5.95</u>	6.92	6.71	5.72
	PIQE↓	55.19	38.04	42.88	31.52	37.67	51.26	36.48	<u>34.78</u>
	MCMA↑	0	0.65	0.65	0.57	0.72	0.57	0.64	<u>0.68</u>
Marsh	NIQE↓	8.14	4.91	5.97	<u>4.86</u>	5.73	5.26	5.19	4.85
	PIQE↓	29.41	22.44	28.69	<u>19.03</u>	29.48	31.31	18.01	26.55
	MCMA↑	0	0.65	0.70	0.61	<u>0.73</u>	0.72	0.55	0.74
House	NIQE↓	2.75	2.40	2.65	<u>2.35</u>	2.37	2.99	2.67	2.29
	PIQE↓	37.33	33.94	31.07	<u>31.51</u>	31.58	41.74	36.55	31.07
	MCMA↑	0	<u>0.69</u>	0.65	0.66	0.68	0.63	0.72	0.68
Woman	NIQE↓	5.96	5.37	5.45	5.91	<u>5.30</u>	5.56	5.42	5.26
	PIQE↓	38.23	34.60	34.21	36.52	<u>32.98</u>	35.14	34.81	<u>32.92</u>
	MCMA↑	0	0.68	0.68	0.56	<u>0.74</u>	0.67	0.64	0.75
Average	NIQE↓	6.1	4.93	5.27	4.92	<u>4.84</u>	5.18	5.00	4.53
	PIQE↓	40.04	32.26	34.21	29.65	32.93	39.86	31.46	<u>31.33</u>
	MCMA↑	0	0.67	0.67	0.6	<u>0.72</u>	0.65	0.64	<u>0.71</u>

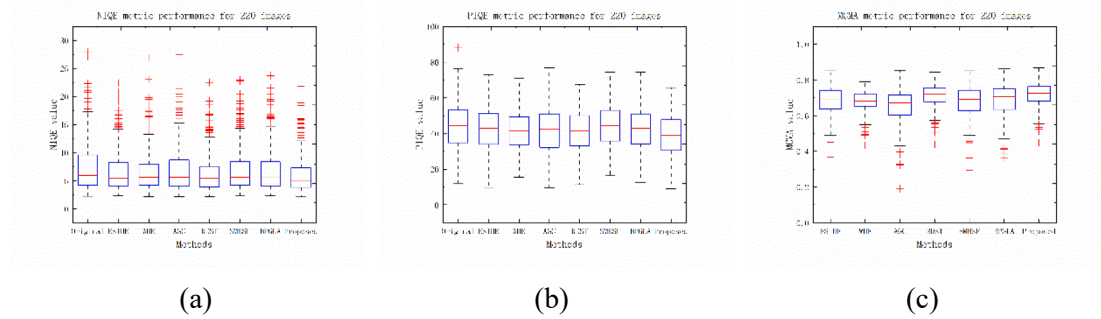


Fig. 16. The comparison results of different metrics for 220 images.

Table 2

Experimental results of computational complexity (Unit: s).

Image index	Size	Time	Image index	Size	Time
Image 1	256 × 256	0.006	Image 6	800 × 600	0.012
Image 2	434 × 381	0.007	Image 7	893 × 600	0.012
Image 3	640 × 480	0.010	Image 8	1000 × 667	0.016
Image 4	750 × 725	0.012	Image 9	1280 × 853	0.020
Image 5	750 × 1000	0.016	Image 10	1556 × 1037	0.029

Table 3

Comparison of different methods on computational complexity (Unit: s).

	256 × 256 (Image 1)	640 × 480 (Image 3)	1000 × 667 (Image 8)	1556 × 1037 (Image 10)
ESIHE	0.003	0.005	0.009	0.018
WHE	0.026	0.034	0.044	0.068
AGC	0.015	0.043	0.087	0.195
RDST	0.008	0.010	0.012	0.017
SMBSF	0.053	0.177	0.357	0.821
BPGLA	0.005	0.008	0.015	0.030
AHEVPC	0.005	0.009	0.014	0.029

images of different sizes, comparable to that of ESIHE, RDST and BPGLA. The majority of its processing time is dedicated to traversing the gamma adjustment coefficient.

5. Conclusion

Existing Histogram Equalization (HE)-based improvement methods fall short in simultaneously addressing the three main limitations of HE: over-enhancement, under-enhancement, and mean shift. Additionally, these methods often overlook the subjective perception of the Human Vision System (HVS). In response, we introduce a systematic approach, Adaptive Histogram Equalization with Visual Perception Consistency (AHEVPC), which is designed to mitigate these shortcomings. Firstly, a CDF-based model is constructed to address the inherent defects of HE. Within this model, we employ dual gamma corrections to mitigate risks of over and under-enhancement effectively. Subsequently, a bias is introduced to one side of the histogram to counteract mean shift. Moreover, to align the subjective and objective effects of the image enhancement process closely, we incorporate an adaptive bias adjustment mechanism, facilitated by the addition of a weighting factor. Additionally, a visibility threshold is applied to constrain the histogram, thereby rendering the final enhanced image more natural and visually appealing. Extensive experimental results demonstrate that our proposed scheme not only broadens the applicability but also surpasses other HE-based methods in delivering superior visual quality. Notably, our algorithm focuses on histogram manipulation without complicating the HE processes, rendering it suitable for real-time image enhancement applications. However, it is observed that images with large flat areas may exhibit undesirable artifacts, marking a potential area for breakthrough advancements in our future research endeavors.

CRediT authorship contribution statement

Qi Yuan: Conceptualization, Data curation, Formal analysis, Investigation, Methodology, Project administration, Resources, Software, Supervision, Validation, Visualization, Writing – original draft, Writing – review & editing. **Shengkui Dai:** Funding acquisition, Project administration, Supervision, Writing – review & editing.

Declaration of competing interest

The authors declare that they have no known competing financial interests or personal relationships that could have appeared to influence the work reported in this paper.

Data availability

The data that has been used is confidential.

Acknowledgment

The authors would like to thank Professor Ma Zhan for his valuable advice and support during the manuscript writing.

References

- [1] B.C. Thai, A. Mokraoui, Tone mapped hdr images contrast enhancement using piecewise linear perceptual transformation. In: 2019 27th European Signal Processing Conference (EUSIPCO), 2019.
- [2] J.-L. Lisani, Adaptive local image enhancement based on logarithmic mappings, in: 2018 25th IEEE International Conference on Image Processing (ICIP), 2018, pp. 1747–1751.
- [3] A. Acharya, A.V. Giri, Contrast improvement using local gamma correction, in: In: 2020 6th International Conference on Advanced Computing and Communication Systems (ICACCS), 2020, pp. 110–114.
- [4] T. Arici, Dikbas, Salih, Altunbasak, Yucel, A histogram modification framework and its application for image contrast enhancement, *IEEE Trans. Image Process.* 18 (9) (2009) 192–1935.
- [5] J. Park, B.-U. Lee, Color image enhancement with high saturation using piecewise linear gamut mapping, *J. Vis. Commun. Image Represent.* 67 (2020) 102759.
- [6] S. Li, W. Jin, L. Li, Y. Li, An improved contrast enhancement algorithm for infrared images based on adaptive double plateaus histogram equalization, *Infrared Phys. Technol.* 90 (2018) 164–174.
- [7] Q. Wang, R.K. Ward, Fast image/video contrast enhancement based on weighted thresholded histogram equalization, *IEEE Int. Conf. Commun.* 53 (2) (2007) 757–764.
- [8] M. Veluchamy, B. Subramani, Image contrast and color enhancement using adaptive gamma correction and histogram equalization, *Optik* 183 (2019) 329–337.
- [9] Y. Kim, Contrast enhancement using brightness preserving bi-histogram equalization, *IEEE Trans. Consum. Electron.* 43 (1) (1997) 1–8.
- [10] Yu. Wang, Q. Chen, Image enhancement based on equal area dualistic sub-image histogram equalization method, *IEEE Trans. Consum. Electron.* 45 (1) (1999) 68.
- [11] S.D. Chen, A.R. Ramli, Contrast enhancement using recursive mean-separate histogram equalization for scalable brightness preservation, *IEEE Trans. Consum. Electron.* 49 (4) (2003) 1301–1309.
- [12] K.S. Sim, C.P. Tso, Y. Tan, Recursive sub-image histogram equalization applied to gray scale images, *Pattern Recogn. Lett.* 28 (2007) 1209–1221.
- [13] C. Shaham, A.K. Nercessian, S.S. Panetta, Agaian, Non-linear direct multi-scale image enhancement based on the luminance and contrast masking characteristics of the human visual system, *IEEE Trans. Image Process.* 22 (9) (2013) 3549–3561.
- [14] I.R. Khan, S. Rahardja, M.M. Khan, M.M. Movania, F. Abed, A tone-mapping technique based on histogram using a sensitivity model of the human visual system, *IEEE Trans. Ind. Electron.* 65 (4) (2018) 3469–3479.
- [15] K.S. Song, M.G. Kang, Optimized tone mapping function for contrast enhancement considering human visual perception system, *IEEE Trans. Circuits Syst. Video Technol.* 29 (11) (2018) 3199–3210.
- [16] G. Jiang, S.C.F. Lin, C.Y. Wong, M.A. Rahman, T.R. Ren, N. Kwok, H. Shi, Y.H. Yu, T. Wu, Color image enhancement with brightness preservation using a histogram specification approach, *Optik-Int. J. Light Electron Optics* 126 (24) (2015) 5656–5664.
- [17] S. Thangavelu, G. Eappen, V. Suresh, A. Rajesh, R. Mageshvaran, Contrast enhancement using quantile separation and bi-histogram equalization. 2019 Innovations in Power and Advanced Computing Technologies, 2019.
- [18] S. Kansal, R.K. Tripathi, New adaptive histogram equalisation heuristic approach for contrast enhancement, *IET Image Proc.* 14 (6) (2020) 1110–1119.
- [19] S.-D. Chen, A. Ramli Rahman, Minimum mean brightness error bi-histogram equalization in contrast enhancement, *IEEE Trans. Consum. Electron.* 49 (4) (2003) 1310–1319.
- [20] M. Kim, M. Chung, Recursively separated and weighted histogram equalization for brightness preservation and contrast enhancement, *IEEE Trans. Consum. Electron.* 54 (3) (2008) 1389–1397.
- [21] A. Singh, S. Yadav, N. Singh, Contrast Enhancement and Brightness Preservation Using Globallocal Image Enhancement Techniques, in, 2016.
- [22] D. Tohl, J.S. Jimmy Li, Image enhancement by s-shaped curves using successive approximation for preserving brightness, *IEEE Signal Process Lett.* 24 (8) (2017) 1247–1251.
- [23] H. Tanaka, A. Taguchi, A contrast enhancement method of only the region of interest while preserving mean brightness. In: 2018 International Symposium on Intelligent Signal Processing and Communication Systems (ISPACS), 2018.
- [24] S. Park, Y. G. Shin, S. J. Ko, Contrast enhancement using sensitivity model-based sigmoid function, *IEEE Access* PP 7 (2019) 161573–161583.
- [25] W.H. Press B.P. Flannery S.A. Teukolsky W.T. Vetterling Numerical Recipes in c: the Art of Scientific Computing (book) 1992 255 270.
- [26] N. Singh, A.K. Bhandari, Image contrast enhancement with brightness preservation using an optimal gamma and logarithmic approach, *IET Image Proc.* 14 (4) (2020).
- [27] C.H. Ooi, N.A. Mat Isa, Quadrants dynamic histogram equalization for contrast enhancement, *IEEE Trans. Consum. Electron.* 56 (4) (2010) 2552–2559.
- [28] K. Singh, R. Kapoor, Image enhancement using exposure based sub image histogram equalization, *Pattern Recogn. Lett.* 36 (2014) 10–14.
- [29] Q. Wang, R.K. Ward, Fast image/video contrast enhancement based on weighted thresholded histogram equalization, *IEEE Trans. Consum. Electron.* 53 (2007).
- [30] M. Hajinorooz, A. Grigoryan, S. Agaian, Image enhancement with weighted histogram equalization and heap transforms, in, World Automation Congress, 2016.
- [31] S.C. Huang, F.C. Cheng, Y.S. Chiu, Efficient contrast enhancement using adaptive gamma correction with weighting distribution, *IEEE Trans. Image Process. A Publ. IEEE Signal Process. Soc.* 22 (3) (2013) 1032–1041.
- [32] S. Rahman, M.M. Rahman, M. Abdullah-Al-Wadud, G.D. Al-Quaderi, M. Shoyaib, An adaptive gamma correction for image enhancement, *Eurasip J. Image Video Process.* 2016 (1) (2016) 35.
- [33] S. Lee, C. Kim, Ramp distribution-based contrast enhancement techniques and over-contrast measure, *IEEE Access* 7 (2019) 73004–73019.
- [34] S.W. Kim, B.D. Choi, W.J. Park, S.J. Ko, 2d histogram equalisation based on the human visual system, *Electron. Lett.* 52 (6) (2016) 443–445.
- [35] Wu. Hao-Tian, M. WeiQi, M. Shuyi, C. Yiu-Ming, T. Shaohua, Reversible data hiding with image contrast enhancement based on two-dimensional histogram modification, *IEEE Access* 7 (2019) 83332–83342.
- [36] D. Kim, C. Kim, Contrast enhancement using combined 1-d and 2-d histogram-based techniques, *IEEE Signal Process Lett.* 24 (6) (2017) 804–808.
- [37] T. Celik, T. Tjahjadi, Contextual and variational contrast enhancement, *IEEE Trans. Image Process.* 20 (12) (2011) 3431–3441.

- [38] A. Ignatov, N. Kobyshev, R. Timofte, K. Vanhoey, Dslr-quality photos on mobile devices with deep convolutional networks, in, IEEE Int. Conf. Comput. Vision (ICCV) 2017 (2017) 3297–3305.
- [39] Y.S. Chen, Y.-C. Wang, M.-H. Kao, Y.-Y. Chuang, Deep photo enhancer: Unpaired learning for image enhancement from photographs with gans, in, IEEE/CVF Conf. Comput. Vision Pattern Recognit. (CVPR) 2018 (2018) 6306–6314.
- [40] S. Moran, P. Marza, S. McDonagh, S. Parisot, G. Slabaugh, Deeplpf: Deep local parametric filters for image enhancement, in, IEEE/CVF Conf. Comput. Vision Pattern Recognit. (CVPR) 2020 (2020) 12823–12832.
- [41] C. Chun-Hsien, Yun-Chin, Li, A perceptually tuned subband image coder based on the measure of just-noticeable-distortion profile, IEEE Trans. Circuits Syst. Video Technol. 5 (6) (1995) 467–476.
- [42] T.-H. Yu J.-M. Dai New Technology of Infrared Image Contrast Enhancement Based on Human Visual Properties 37 2008 951 954.
- [43] A. Mittal, R. Soundararajan, A.C. Bovik, Making a “completely blind” image quality analyzer, IEEE Signal Process Lett. 20 (3) (2013) 209–212.
- [44] N. Venkatanath, D. Praneeth, S.S. Maruthi Chandrasekhar Bh, S.S. Channappayya, Medasani, Blind image quality evaluation using perception based features, 2015.
- [45] M. Abdoli, F. Nasiri, P. Brault, M. Ghanbari, A quality assessment tool for performance measurement of image contrast enhancement methods, IET Image Proc. 13 (5) (2019) 833–842.
- [46] A. Weber, The usc-sipi image database, [DB/OL], <http://sipi.usc.edu/database/> (1977).
- [47] X. Guo, Y. Li, H. Ling, Lime: Low-light image enhancement via illumination map estimation, IEEE Trans. Image Process. 26 (2) (2016) 982–993.
- [48] D. M. Pablo Arbelaez, Charless Fowlkes, The berkeley segmentation dataset and benchmark, [DB/OL], <https://www2.eecs.berkeley.edu/Research/Projects/CS/vision/grouping/segbench/> (2007).
- [49] Shuhang, Wang, Jin, Zheng, Hai-Miao, Hu, Li, Naturalness preserved enhancement algorithm for non-uniform illumination images., IEEE transactions on image processing : a publication of the IEEE Signal Processing Society 22 (9) (2013) 3538-48.
- [50] V. Bychkovsky, S. Paris, E. Chan, F. Durand, in: Learning photographic global tonal adjustment with a database of input/output image pairs, The Twenty-Fourth IEEE Conference on Computer Vision and Pattern Recognition, 2011, pp. 97–104.